Marine Geophysical Research (2019) 40:223–235
https://doi.org/10.1007/s11001-018-9359-2

ORIGINAL RESEARCH PAPER

Upper Miocene–Pliocene provenance evolution of the Central Canyon in northwestern South China Sea

Yuchi Cui[1] · Lei Shao[1] · Peijun Qiao[1] · Jianxiang Pei[2] · Daojun Zhang[2] · Huyen Tran[3]

Received: 31 October 2017 / Accepted: 24 May 2018 / Published online: 5 June 2018

Abstract

Provenance studies of the Central Canyon, Qiongdongnan Basin has provided significant insights into paleographic and sedimentology research of the South China Sea (SCS). A suite of geochemical approaches mainly including rare earth elemental (REE) analysis and detrital zircon U–Pb dating has been systematically applied to the "source-to-sink" system involving our upper Miocene–Pliocene Central Canyon sediments and surrounding potential source areas. Based on samples tracing the entire course of the Central Canyon, REE distribution patterns indicate that the western channel was generally characterized by positive Eu anomalies in larger proportion, in contrast to the dominance of negative values of its eastern side during late Miocene–Pliocene. Additionally, for the whole canyon and farther regions of Qiongdongnan Basin, the number of samples bearing negative Eu anomalies tended to increase within younger geological strata. On the other hand, U–Pb geochronology results suggest a wide Proterozoic to Mesozoic age range with peak complexity in Yanshanian, Indosinian, Caledonian and Jinningian periods. However in detail, age combination of most western samples displayed older-age signatures than the eastern. To make it more evidently, western boreholes of the Central Canyon are mainly characterized with confined Indosinian and Caledonian clusters which show great comparability with mafic-to-ultramafic source of Kontum Massif of Central Vietnam, while eastern samples largely bear with distinguishable Yanshanian and Indosinian peaks which more resemble with Hainan Island. Based on geochemistry and geochronology analyses, two significant suppliers and sedimentary infilling processes are generated: (1) the Indosinian collision orogenic belt in central-northern Vietnam, Indochina has ever played significant role in Central Canyon sedimentary evolution, (2) Hainan Island once as a typical provenance restricted within eastern Central Canyon, has been enlarging its influence into the whole channel, even into the farther western regions of Qiongdongnan Basin.

Keywords South China Sea · Upper Miocene–Pliocene · Provenance · Rare earth elements · Zircon U–Pb dating

Introduction

Reservoir quality of sandstones is critically impacted with the clastic composition controlled by provenance distribution patterns. Therefore, potential sources and sedimentary transporting routes of the northern South China Sea (SCS) are of remarkable significance on hydrocarbon exploration as well as on geological information archive, such as paleoenvironmental changes and tectonic evolution (Fig. 1a) (Morton et al. 2001; Rossi et al. 2002). Nevertheless, it virtually remains further investigation due to the complexity of geological framework, limited borehole coverage and poorly dated stratigraphy in this region, particularly northwestern SCS area. Submarine canyons, which strongly dissect continental margins, are commonly regarded as significant conduits for sediment transfer from continental shelf into

Electronic supplementary material The online version of this article (https://doi.org/10.1007/s11001-018-9359-2) contains supplementary material, which is available to authorized users.

✉ Lei Shao
lshao@tongji.edu.cn

[1] State Key Laboratory of Marine Geology, Tongji University, 1239 Siping Road, Shanghai 200092, China

[2] Zhanjiang Branch of China National Offshore Oil Corporation, Zhanjiang 524057, Guangdong, China

[3] Hanoi University of Mining and Geology, Hanoi, Vietnam

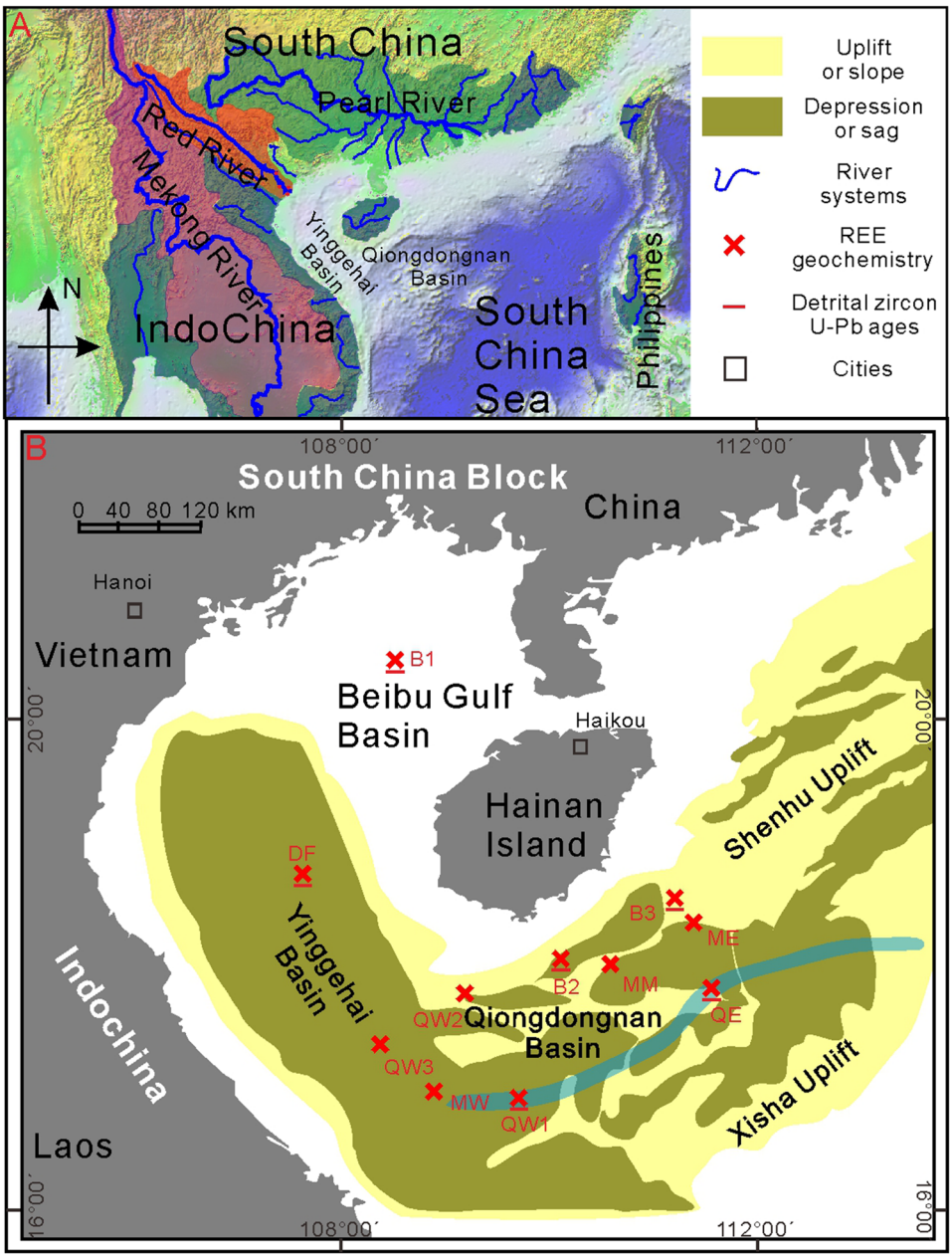

Fig. 1 **a** Topographic map of the Yinggehai and Qiongdongnan Basins relative to Southeast Asia and the South China Sea (SCS) and the bottom zoomed plot. **b** The special tectonic units, studied borehole samples and published data. Crosses and lines represent the analyzed samples of rare earth element (REE) and detrital zircon U–Pb dating, respectively

deep-sea basins (Popescu et al. 2004; Antobreh and Krastel 2006; Harris and Whiteway 2011). As important hydrocarbon reservoirs, these canyons or channels possess the potential of accumulating huge amount of sandy deposition, which have always attracted widespread interests all over the world (Mayall et al. 2006; Gong et al. 2011). Globally, sediments transported in canyon systems not only gathered voluminous oil and natural gas resources, but also kept high-quality record of regional structural evolution, environmental and climatic change information (Hale et al. 2014; Bayliss and Pickering 2015; Flecker et al. 2015; Reimchen et al. 2016). Enhanced understanding of these geological structures on morphology, composition, evolution as well as depositional dynamics has been greatly generalized resulting from high-resolution seismic data and sequence stratigraphy (Arzola et al. 2008; Mountjoy et al. 2009; Jobe et al. 2011).

The present "S-shaped" Central Canyon is a large axial submarine system with an approximate length of 570 km and width of ~9–30 km, which lies paralleled to the shelf break and stretches with a NE–NEE orientation in the northwestern margin of the SCS (Fig. 1b). Due to its unique internal architecture and interplay of erosion and aggradation processes, forming mechanisms and sedimentary provenances of the Central Canyon area have long been in debate over the past 10 years (He et al. 2013). It has been implied that sufficient sediments for the initial growth of Central

Canyon were provided by rapid and broad Tibetan Plateau uplift around 5.5 Ma (Gong et al. 2011). Meanwhile, the Red River Fault movement also induced high-energy gravity flows providing voluminous material (Yuan et al. 2009). By contrast, Li et al. (2017a) favored that eastern Vietnam has already delivered sufficient sediments with large-scale submarine fans stepwise developing in Central Canyon since 10.5 Ma. Based on further integration and compilation of 2D/3D seismic and well log profiles, provenance evolution was reconstructed for different segments in the Central Canyon source-to-sink system (Su et al. 2013; Li et al. 2017b). After describing morphological characteristics and dissecting internal architectures of the Central Canyon system, Su et al. (2013) developed multi-phases including initial, eroded infilling, tranquil infilling and rejuvenation period in order to reconstruct provenance evolution. On one hand, northern continental slope and major potential sources including Red River, eastern Vietnam or Hainan Island were dominant suppliers to the northwestern SCS, on the other hand, Qiongdongnan tectonic transformation was likely to constrain the evolution of Central Canyon eastern segment around 11.6 Ma (Xie et al. 2006, Su et al. 2014). However, due to lack of convincible evidence requested by source-to-sink system analysis, temporal and spatial variations of sediment composition patterns in Central Canyon area since late Miocene are still perplexing issues from the prospective of origination and infilling mechanisms, which seem even harder to be deeply interpreted by the complicated potential sources adjacent to Yinggehai–Qiongdongnan Basin illustrated in detail as follows. Although details on provenance of Red River remain controversial, its modern drainage system has been revealed as maximum discharge delivering high volumes of sediments into the northwestern SCS during the Neogene, likewise, the paleo–Red River was also presumed to be a significant source (Clift et al. 2006; Milliman and Farnsworth 2011; Zhao et al. 2015). Seismic profiles initially indicated that progradational slope clinoforms were not largely generated in Hainan Island until the late Cenozoic (Van Hoang et al. 2010; Xie et al. 2008). Verified by U–Pb age dating, Hainan Island has already exerted its impact on sediment supply to its adjacent basins during Oligocene–Miocene (Shao et al. 2016; Yan et al. 2011). Additionally, eastward progradation from the Vietnamese margin into the western Qiongdongnan Basin and low degree of weathering conditions from geochemistry analysis together imply a Central Vietnam provenance since the Miocene, which is contrast to the speculation of little sediment delivery due to absorption of the Mekong River drainage basin (Ma et al. 2016). A series of intensive local mafic volcanic activities was also indicated by mineral assemblage of augite and olivine and positive Eu anomalies in the Qiongdongnan Basin during late Cenozoic (Fyhn et al. 2009; Zhao et al. 2015). Similarly, how exactly this suite of provenances influenced the Central Canyon's sedimentary evolution since its origination is scarcely systematically discussed and remains rather elusive.

Provenance studies of sedimentary sequences are critical to basin history analysis and natural resource exploration. It is ineffectively to interpret the source-to-sink system solely based on traditional petrography or heavy minerals particularly in the complicated source areas. Zircon is uniquely characterized by its mineral stability which can withstand mixed effects of weathering, erosion as well as thermal alteration processes (Kosler 2003). Due to its stable isotopic system under different pressure, temperature and fluid composition conditions (Moecher and Samson 2006), detrital zircon U–Pb age spectra dated by Laser Ablation Induction Coupled Plasma Mass Spectroscopy have been increasingly considered as a valuable tool in wide range of geological researches (Cao et al. 2018; Horton et al. 2008; Condie et al. 2009). In addition to zircon U–Pb geochronology, immobile trace elements, especially rare earth elements (REE) are also robust indicators of source rock geochemistry as these elements suffer minor modification from sorting, fractionation and diagenesis processes during transportation (Shao et al. 2017; Mclennan 1989). Although detrital single-grain analysis has gained much popularity among provenance studying field, bulk rock geochemistry is still able to provide quantitative insights into siliciclastic sediments.

In this study, we aim to address the following problems by focusing on new results of detrital zircon U–Pb ages and geochemical analysis from Yinggehai Basin and Qiongdongnan Basin, in comparison with recalculation and integration on published or unpublished data from Central Vietnam, modern Red River, Hainan Island and SCS basement: (1) what exactly are the sediment contributors surrounding the SCS for the Central Canyon and what types of clastic materials did they provide? And (2) what is the sedimentary infilling history for the entire Central Canyon during late Miocene–Pliocene?

Geological setting

Basically, Yinggehai Basin is located between Hainan Island and Indochina block with a NNW–SSE orientation. Perpendicular to the trend of Yinggehai Basin, Qiongdongnan Basin is surrounded by Hainan Island, Xisha Uplift and Shenhu Uplift (Fig. 1b). Both tectonic evolution and stratigraphic structures of Yinggehai and Qiongdongnan Basin have been investigated for decades. Mechanisms including the strike-slip events of the Red River Shear Zone, the Indochina Block extrusion model and the SCS seafloor spreading have been debated but remain disputed for the interpretation of these two oceanic basins' evolutionary histories (Zhu et al. 2009; Zhang et al. 2013; Zhu and Lei 2013). Nevertheless,

typical passive continental margins of Yinggehai–Qiongdongnan Basin have still been identified: a large-scale rifting stage prior to the late Oligocene and a post-rifting stage with accelerated thermal subsidence since early Miocene (Taylor and Hayes 1983). In particular, intensive tectonic activities of the Red River Fault Zone took place during the Neogene post-rifting phase when the previous strike-slip reversal processes had been switched into dextral movement in the northern Vietnam (Rangin et al. 1995). This could somehow modify or change the characteristics of the parent rocks exposed in this area. Meanwhile as additional complementary information, Neogene magmatism proved to be relatively strong around the SCS continental margins. Widely distributed basalts along the central and southern Indochina block and basaltic extrusions on Hainan Island were also explicitly recorded (Yan et al. 2006). Under controlled by this complexity of the tectonic backgrounds, littoral to neritic sedimentary environment has gradually been changed into bathyal to abyssal facies since late Miocene in most regions of the Qiongdongnan Basin where submarine fans or deltas were abundantly generated. On the other hand, shelf–slope systems were partly distributed in the Yinggehai Basin facilitated by high rate of sediment supply (Cai et al. 2013; Zhang et al. 2015; Li et al. 2016). In this deep-water sedimentary setting, the main drainages of Central Canyon transporting sediment material through Qiongdongnan abyssal plains were initially developed (Fig. 2).

Analytical methods

Detrital zircon U–Pb dating implies the time of zircon growth, which is generally the rock crystallization age. The zircon U–Pb system is particularly characterized by a high closure temperature and in most cases unaffected by high-grade metamorphism to temperatures at least as high as 750 C (Cherniak and Watson 2001; Carter and Bristow 2015). Extensive oil and gas drilling programs have been conducted in the northern SCS area by China National Offshore Oil Corporation (CNOOC). Specific sample locations in our research are displayed in Fig. 1b, with detailed sampling information provided in Table 1. Age models of all these boreholes are derived from biostratigraphical and unpublished seismic data owned by CNOOC. Zircons in our samples were extracted from the bulk sediments by conventional magnetic and heavy liquid separation techniques in laboratory of the Institute of Regional Geology and Mineral Resources, Hebei Province, China. Prior to analysis, zircon grains have been randomly selected followed by cathodoluminescence (CL) imaging on the polished epoxy

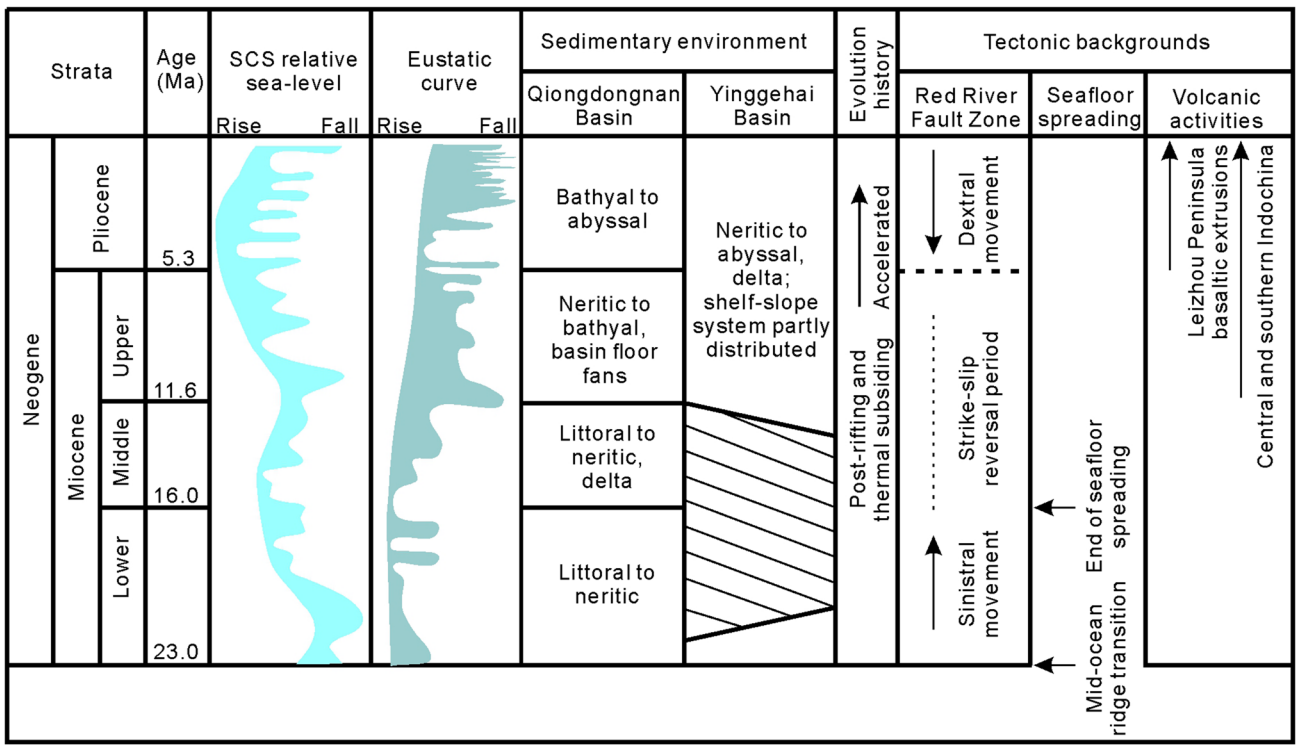

Fig. 2 Schematic stratigraphic column of the major northern SCS basins (Mi and Zhang 2011) with relative and global sea-level variations (Haq 1988), sedimentary environment, SCS evolution history (Li et al. 2016) and tectonic backgrounds (Taylor and Hayes 1983; Leloup et al. 1995; Yan et al. 2006)

Table 1 Stratigraphic position of analyzed samples in this study and published research (Wang et al. 2014; Cao et al. 2015)

Borehole	Geographical location	Sample name	Strata	Analytical depth (m)/sample number			
				REE geochemistry	References	U–Pb dating	References
DF	Yinggehai Basin	DF-1	Pliocene	900-2392/31	This study	1105-2193/5	Wang et al. (2014)
		DF-2	Upper Miocene	2422-3234/12	This study	2600-2898/3	Wang et al. (2014)
QW1	Qiongdongnan Basin	QW1-1	Pliocene	2205-3748/363	This study	2665-3666/3	This study
		QW1-2	Upper Miocene	3750-4000/126	This study	3766-3950/3	This study
QW2	Qiongdongnan Basin	QW2-1	Pliocene	960-1810.5/25	This study		
		QW2-2	Upper Miocene	1844-2020.8/7	This study		
QW3	Qiongdongnan Basin	QW3-1	Pliocene	1500-3610/48	This study		
		QW3-2	Upper Miocene	3640-4124/21	This study		
QE	Qiongdongnan Basin	QE-1	Pliocene	2510-3065/112	This study	58	This study
		QE-2	Upper Miocene	3070-3630/120	This study	3276/1	Cao et al. (2015)
MW	Qiongdongnan Basin	MW	Middle Miocene	3430-3616/5	This study		
MM	Qiongdongnan Basin	MM	Middle Miocene	2910-3255/11	This study		
ME	Qiongdongnan Basin	ME	Middle Miocene	2660/1	This study		
B1	Beibu Gulf Basin	B1	Basement	1440-1490/3	This study	1490/1	This study
B2	Qiongdongnan Basin	B2	Basement	2700/1	This study	2700/1	This study
B3	Qiongdongnan Basin	B3	Basement	2146-2326/3	This study	2166-2326/3	This study

disks to locate proper analytical spots in oscillatory zoning (Supplementary Fig. S4 for CL images). The U–Pb isotopic dating was processed by laser ablation–inductively coupled plasma–mass spectroscopy (LA–ICP–MS) at the State Key Laboratory of Marine Geology, Tongji University, China. The instrumentation involves a Thermo Elemental X-Series ICP–MS coupled to a New Wave 213 nm laser ablation system, of which the laser beam has been set to a 10 Hz repetition rate with a spot size of 30 μm. The ablated material was then transported into the ICP–MS with a He–Ar gas mixture. 20 s of gas blank was incorporated for each analysis before 50 s duration of data acquisition. Our method employs an external standard zircon 91500 (1065.4 ± 0.3 Ma) analyzed twice every seven analyses (Wiedenbeck et al. 1995) and Plešovice (337.1 ± 0.4 Ma) for accuracy calibration (Sláma et al. 2008). The U–Pb ages were finally reported with 1σ level of uncertainty calculated by ICPMSDATACAL combined with the common Pb correction (Supplementary Table S1, 2; Supplementary Fig. S5) (Andersen 2002; Liu et al. 2010), while visualization for age distribution patterns were achieved via histograms and kernel density estimation plots (Vermeesch 2012). Generally, $^{206}Pb/^{238}U$ ages are more precise for younger ages (< 1000 Ma), whereas $^{207}Pb/^{206}Pb$ ages are applied for older ages (> 1000 Ma).

Sediments aimed for REE analysis were first washed with deionized distilled water at the State Key Laboratory of Marine Geology, Tongji University, China. After being dried at 50 °C for 48 h and crushed in an agate mortar, about 3 g of dry powdered samples were heated to 600 °C for 2 h and then digested with 0.1 M HCl in order to remove organic matter and interlayer water as well as small part of marine carbonates, separately. Dissolved in a HF–HNO_3 mixture, trace elements were measured using Thermo Elemental X-Series (ICP–MS). Certified standards including GSR-5, GSR-6 and GSD-9 provided by the Institute of Geophysical and Geochemical Exploration, China, have been repeatedly analyzed as unknown samples for the precision and accuracy assessment. The external precision (1σ) was generally better than 5% and our reported concentrations turned out to be in consistent with the recommended data (Supplementary Table S3). The measured REE abundances have been normalized to the chondrite average (Boynton 1984).

Results

In our study, Yinggehai–Qiongdongnan samples display typical temporal and spatial variations from east to west in upper Miocene–Pliocene (Fig. 3; data of Th/U against ages for Supplementary Fig. S6). Generally, representative tectonic periods are divided into Himalayan (~ present-66 Ma), Yanshanian (~ 135–205 Ma), Indosinian (~ 205–257 Ma), Hercynian (~ Veriscan) (257–386 Ma), Caledonian (~ 400–570 Ma), Jinningian (~ 1000–1400 Ma) and Lvliangian (~ 1800–2500 Ma) movements. In the westernmost studied areas, both DF-1 and DF-2 are similarly observed with rather broad age spectra covering Yanshanian, Indosinian, Caledonian, Jinningian even Lvliangian peaks. Compared to DF-1, Pliocene sample of DF-2 displays Indosinian cluster (~ 235 Ma) of larger proportion within its overall pattern. As for another two Qiongdongnan boreholes, age combination differences among separate samples are more

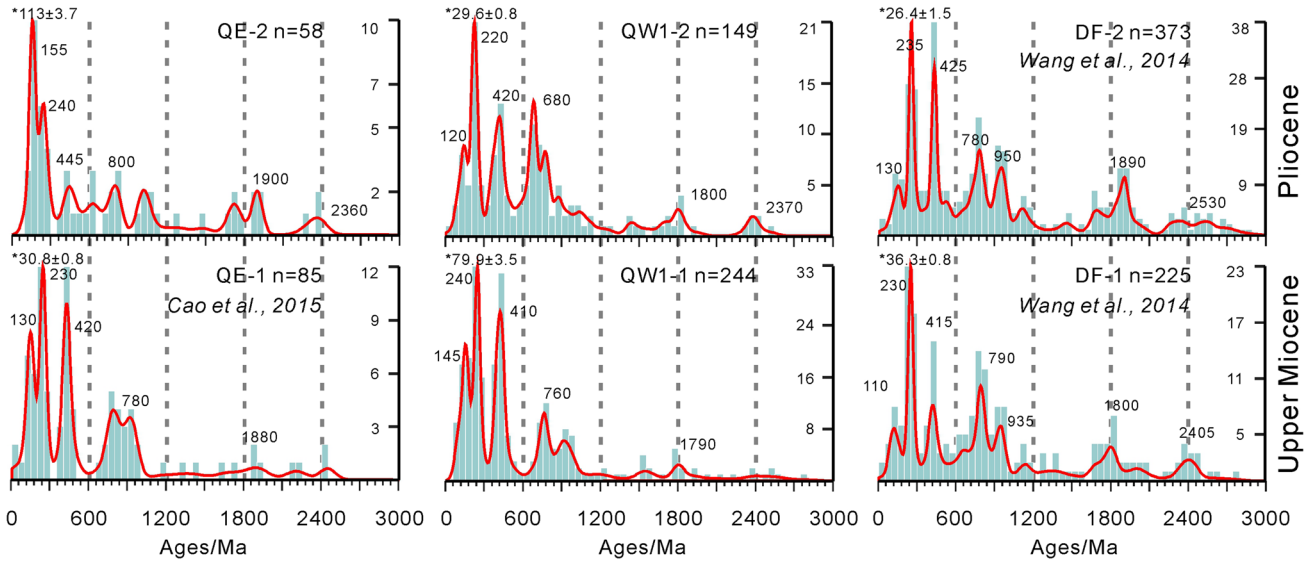

Fig. 3 Histograms and probability density distribution plots for detrital zircon U–Pb ages of the Yinggehai–Qiongdongnan Basin samples from upper Miocene to Pliocene with typical age peaks numbered (Ma). The youngest zircon U–Pb age (Ma) is marked with * in the upper left corner. n represents the number of concordant analyses relative to all grains. Published data in Dongfang gas field of Yinggehai Basin from Wang et al. (2014) and data in Qiongdongnan Basin from Cao et al. (2015) have been renamed and displayed on plot for comparison

clearly identified. For well QW1 further proximal to Central Vietnam, although showing multiple peaks from upper Miocene to Pliocene, QW1-1 is characterized by its Indosinian (240 Ma) and Caledonian (410 Ma) peaks of almost same proportion, while QW1-2 is apparently dominated by its Indosinian (220 Ma) population with the Caledonian (420 Ma) sharply decreased and Jinningian (680 Ma) largely increased. Comparatively, borehole QE in the easternmost is also identified for weaker Caledonian signal (445 Ma) within younger strata sediments of QE-2. Moreover, both QE-1 and QE-2 are commonly featured by their higher Yanshanian peaks than the other analyzed wells. It should also be noted that the 155 and 240 Ma age peaks of QE-2 have already become the dominant clusters while the rest populations of 445 and 800 Ma have shrunken into secondary proportion.

Figure 4 has provided abundant geochemical information on samples along Central Canyon drainage area. With all studied wells roughly considered, light rare earth elements (LREE) enrichment is evidently identified in all borehole samples. Especially among upper Miocene–Pliocene wells including DF, QW3, QW1 and QE, a decreasing trend in both values and numerals of positive Eu anomalies is discerned eastwards. In detail, well DF in northwestern Yinggehai Basin displays pronounced positive Eu anomalies within almost all the layers with only one slight positive value detected in samples (1506–2030 m) of DF-2. To the further east, the slight negative Eu anomaly is first observed in Pliocene samples (1500–1865 m) of QW3-2 in spite of obvious positive Eu anomalies for its other layers. Difference between upper Miocene and Pliocene sample for QW1 is more apparent. No negative anomalies are identified in QW1-1 while upper-layer samples in QW1-2 are featured by moderate-to-obvious negative values. As for the easternmost well, nearly all the QE samples are exclusively characterized by negative Eu anomalies except for the only slight positive data within 3070–3168 m. Contrast to resemblance with PAAS for other boreholes, QW2 located closer to Hainan Island exhibits larger disparity with PAAS pattern. Moreover, vertically, QW2-2 shares relatively higher-level of similarity to PAAS with larger overall REE concentration than QW2-1. However, most samples of QW2 are exhibiting intensive Eu depletion with the only slight positive data within 960–1100 m. Additionally, as complementary evidence, middle Miocene samples including MW, MM and ME also display remarkable spatial shifting in Eu anomalies. MW lying in the westernmost is featured by highest positive value while ME to the east shows strong negative signal.

Discussion

Provenance hypotheses

Geographical location of the Central Canyon indicates primary potential provenances including the modern Red River drainages, Kontum Massif of Central Vietnam areas, Hainan Island, SCS basement and other possible source suppliers (Fig. 5). Abundant zircon U–Pb dating and REE

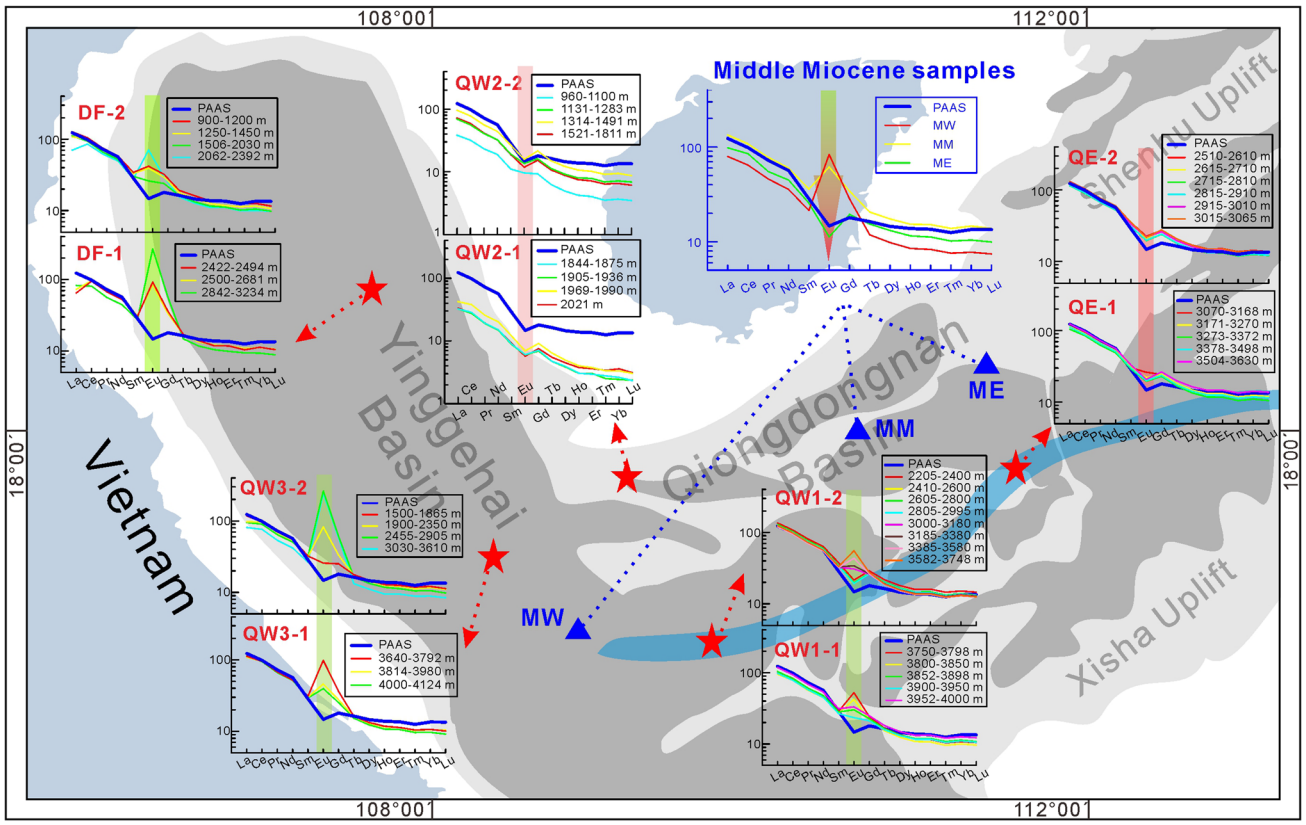

Fig. 4 Chondrite normalized REE patterns of upper Miocene–Pliocene samples in the study area; Eu anomaly values are highlighted on the plot

geochemical data on bedrocks and sediments of Indochina, South China blocks, surrounding fluvial networks and northern SCS basement has made great contributions to constraining the age distribution patterns of those potential source areas. Specifically, Eu anomalies are ubiquitously utilized in provenance discrimination studies as mafic or ultramafic rocks are typically featured by positive values while acidic or sedimentary rocks usually generate the opposite results. Therefore, by comparing zircon ages and REE patterns in the source-to-sink system, the Central Canyon sedimentary infilling evolution could be better interpreted. However, it should still be considered cautiously due to possible sedimentary mixing effect from various end members.

Modern Red River extends along the Ailao Shan–Red River Fault Zone, whose upstream bedrocks are mainly comprised of Mesozoic sedimentary rocks while downstream is ubiquitously featured by schists and gneisses (Fig. 5) (Leloup et al. 1995). Particularly, age signatures of the Red River might be imprudently analyzed, as its paleo-drainage courses may have suffered drastic changes from the East Asia tectonic activities, such as Tibetan uplift. Possible upstream capturing over the Cenozoic was likely to take place to change the sediment supply of the paleo–Red River (Clark et al. 2004). Hence, U–Pb chronology data cited in this paper only represents its modern topographic framework. Due to wide drainage areas, great lithological complexity and severe geotectonic modification, a broad age range (~2500–30 Ma) with apparent Indosinian and Jinningian peaks are identified (Van Hoang et al. 2009). To be addressed, there is a unique Himalayan cluster (~30 Ma) in its multimodal U–Pb combination compared to age patterns of other sources.

Central Vietnam of the Indochina block is widely occupied by Paleozoic–Mesozoic sedimentary rocks and mafic-to-ultramafic bedrocks (Fig. 5). Obviously, its Indosinian–Variscan (260 Ma) and Caledonian (430 Ma) peaks are almost of same proportion combined with a relatively smaller Jinningian cluster (945 Ma) (Burrett et al. 2014). Large-scale submarine fans were confirmed by seismic profiles and heavy mineral analysis on the deepwater sediments of Dongfang gas field, Yinggehai Basin, which evidently indicate a critical contribution from Kontum Massif of Central Vietnam (Zhong et al. 2013). According to previous studies, the Indochina Block experienced drastic extruding and deforming processes during late Triassic, resulting in high volumes of Paleozoic even Proterozoic zircon grains in the Central Vietnam sediments and thick successions in SCS basins. With continual Tethyan subduction beneath Eurasian Plate, extensive magmatic activities were especially taking

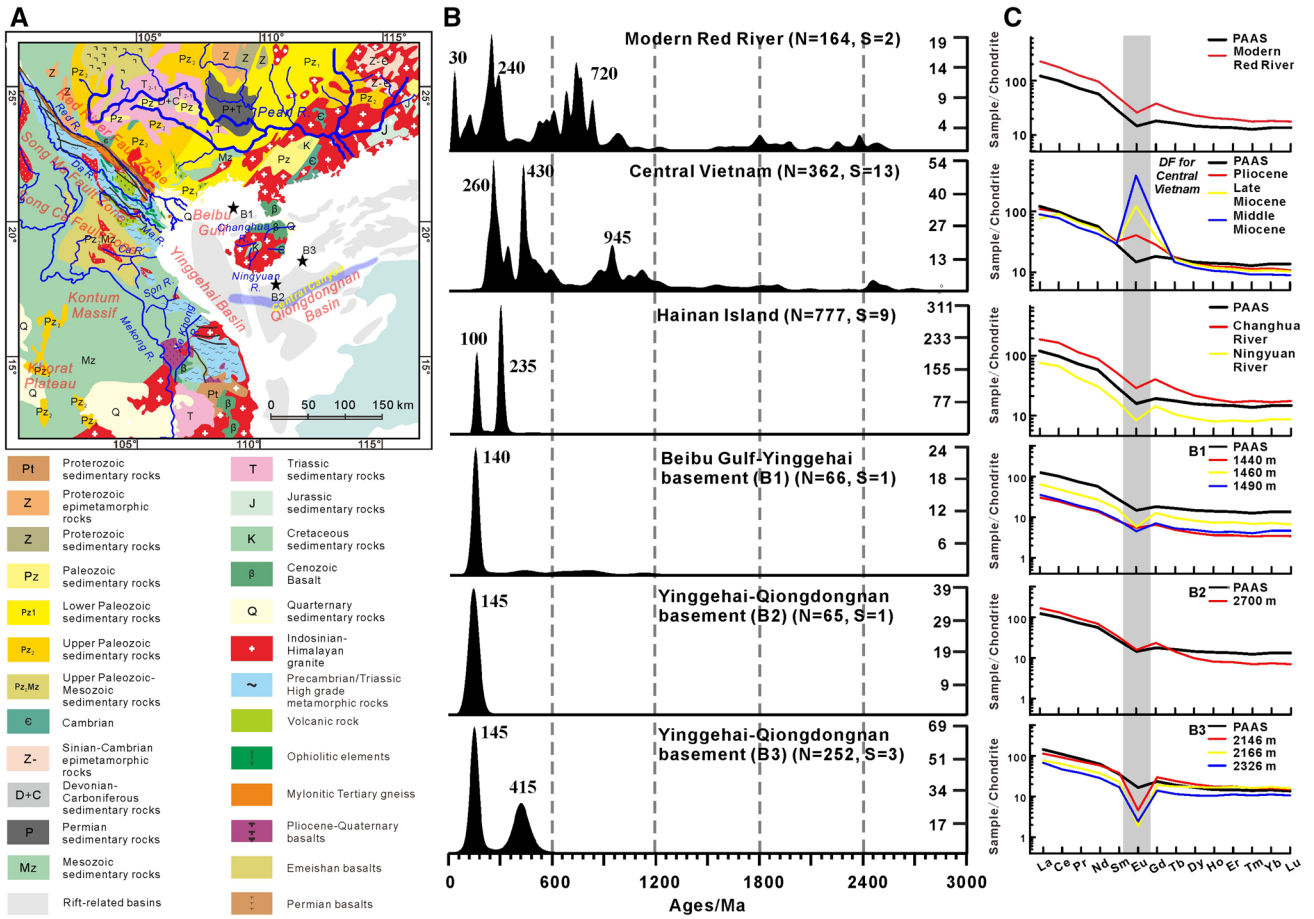

Fig. 5 **a** Simplified geological map of the potential source areas with tectonic units including Yinggehai Basin, Qiongdongnan Basin, Red River Fault Zone, Song Ma Fault Zone, Song Ca Fault Zone, Kontum Massif and Khorat Plateau (based on the geological map of Asia 1975, Chinese Academy of Geological Sciences, 1975). Major drainage systems include Red River, Mekong River, Changhua River and Ningyuan River (Zeng and Zeng 1989; Li et al. 2012). **b** Compilation of published and unpublished detrital zircon U–Pb ages are displayed for different potential source areas (Van Hoang et al. (2009) for modern Red River; Burrett et al. (2014) for Central Vietnam; Xu et al. (2014), Cao et al. (2015) and Wang et al. (2015) for Hainan Island). *S* number of samples, *N* number of concordant analyses. **c** REE distribution patterns for potential sources are also shown (Zhao et al. (2015) for modern Red River; Shao et al. (2010) for Hainan Island)

place during Indosinian movement leading to a relatively high peak of 260 Ma. In the following Cenozoic period, this potential source might be partially modified under the influence from the activity of Red River, Song Ma and Song Ca Fault Zones (Kesselmans et al. 2001; Usuki et al. 2009). Consequently, the age signatures with three well-defined U–Pb peaks for this potential mafic-to-ultramafic sediment contributor kept a good record of the regional tectonic evolution history. As previously mentioned, albeit exhibiting similar wide Indosinian and Jinningian peaks, modern Red River is discriminative from Central Vietnam for its Himalayan cluster (~ 30 Ma) and lack of obvious Caledonian populations (~ 430 Ma). Since Cenozoic tectonic movement had a limited influence on Central Vietnam area, this contributor is devoid of zircons with rather young ages.

According to historical data report, Qiongdongnan and Yinggehai Basins seem to be primary adjacent areas receiving input from Hainan Island due to its relatively steep hillsides and huge-volume runoff (Zeng and Zeng 1989). Changhua and Ningyuan River are two important rivers generated from the central mountains down to surrounding plains (Fig. 5). Parent rocks of Hainan Island are mainly exposed of intermediate–acidic intrusions with limited modern-age basalts in its northern areas. With regard to the U–Pb signatures, Hainan Island displays well-shaped bimodal pattern clustering at Yanshanian (100 Ma) and Indosinian (235 Ma) periods, which is totally different from modern Red River and Central Vietnam.

Compared to multimodal or bimodal U–Pb combinations of peripheral suppliers, the wide northwestern SCS basement shows relatively simple age signatures. B1 is located in Beibu Gulf Basin while B2 and B3 lie in the middle Qiongdongnan Basin. These three samples are all apparently dominated by the confined Yanshanian peak (~ 140–145 Ma).

As facilitated evidence, Zhu et al. (2017) confirmed the late Jurassic metamorphic basement around Xisha Uplift, which was then intruded by early Cretaceous granitic magmatic bodies. Slightly different from B1 and B2, B3 near to Shenhu Uplift exhibits an additional smaller Caledonian peak (~415 Ma) on its age spectrum.

As REE pattern proves to be a vigorous indicator for provenance studies, geochemical analyses of the potential contributors are also systematically conducted, accordingly. Interestingly, modern Red River, Hainan Island and SCS basement share high-level similarity bearing with negative Eu anomalies and LREE enrichment (Fig. 5). Their overall REE patterns are comparable to PAAS representing acidic or sedimentary rock types. By contrast, borehole DF on the submarine delta is uniquely characterized by strong Eu enrichment since middle Miocene. Since this borehole lies rather close to the continental margin and also confined by seismic profiles, its REE patterns might be reflective of abundant basic terrigenous materials from the contiguous block of Central Vietnam.

Provenance evolution of Central Canyon

As potential source areas assessed in the former section, previous studies indicated that Mesozoic suturing along Indochina–Yangtze boundary turned to be one of the most significant events, which had been defined as the Indosinian orogeny. This crucial movement not only includes multiple-stage subduction and collision processes but widespread igneous activities and subsequent metamorphism and deformation. Specifically, huge serpentinite bodies in Kontum Massif of Central Vietnam representing a remnant of paleo-oceanic between Indochina and South China were exposed in abundance during this period (Trung et al. 2006; Liu et al. 2015), which was then proved to be a substantial mafic-to-ultramafic supplier to the western SCS basins. Accordingly, geochemical results of middle Miocene samples of MW, MM and ME tracing the Central Canyon course strongly imply the unbalanced distribution of basic sediments in Qiongdongnan Basin prior to late Miocene. MW nearest to the Vietnamese margin received much larger volume of basic material than the other two wells close to Hainan Island which provided acidic type of sediments. Naturally, highest positive Eu anomalies were observed in its REE pattern. Basically, implication could be made that influence of mafic-to-ultramafic sediments from Kontum Massif on Central Canyon might be weakened or diluted when transported eastward (Fig. 4).

Based on compilation of previous geochronologic analysis, detrital zircon U–Pb ages have revealed a stable provenance of the upper Miocene to Pliocene sediments west of the Central Canyon drainage. Three broad age groups corresponding to Indosinian, Caledonian and Jinningian events in well DF show high compatibility with U–Pb signatures of Central Vietnam (Fig. 3). Meanwhile, the remarkable positive Eu anomalies for both DF samples also suggest clastic materials in northern Yinggehai Basin principally and continually derived from Kontum Massif basic rock regions (Fig. 6). In addition, although being detected in an extremely small scale, both Himalayan (~30 Ma) and Lvliangian peaks

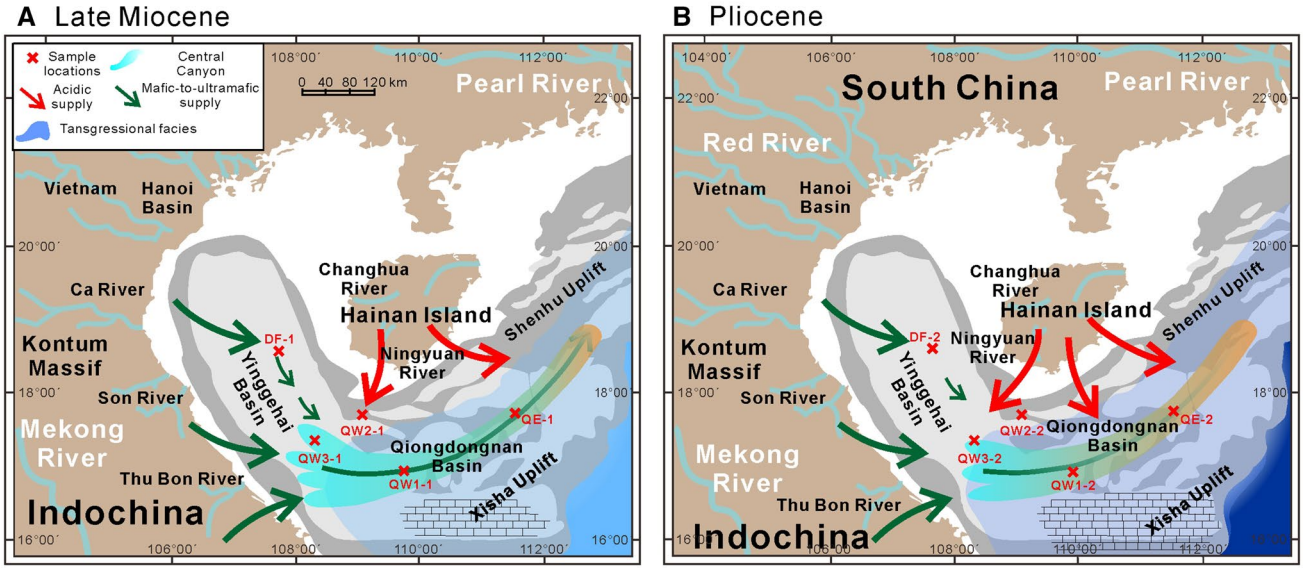

Fig. 6 Schematic source-to-sink evolution model for the late Miocene–Pliocene Yinggehai–Qiongdongnan Basin with Central Canyon highlighted. Arrows stand for sediment transportation routes from different potential source areas to the studied locations. Cyan—areas tend to be more influenced from basic rock sources; orange—areas tend to be more influenced from acidic or sedimentary rock sources

(~2500–1800 Ma) become larger in proportion for Pliocene sample of DF-2, which resemble with modern Red River characteristics to a certain degree. Despite a dominant contribution from the erosion off Kontum Massif highland, this slight change in U–Pb pattern might suggest stronger influence of other secondary sources controlled by Cenozoic tectonic modification processes, such as Red River Shear Zone activities. As confirmed by Chen et al. (2015), appearance of 30 Ma age peak is consistent with the timing of tectonothermal events around Red River Fault Zone.

QW1 and QE confined by geochemical analysis and zircon U–Pb dating are located in the western and eastern part of Central Canyon, separately (Figs. 3, 4). Spatially, both QW1-1 and QE-1 are characterized by obvious similarity to the age signatures of Central Vietnam, displaying high broad Indosinian, Caledonian and Jinningian peaks. Distinct from DF samples discussed above, Yanshanian clusters are also clearly identified indicating non-neglectable clastic materials from other important provenances. Since Hainan Island is featured by unique bimodal pattern with large Yanshanian and Indosinian peaks, sediments might be eroded from its central highs down into the north of Central Canyon channel. Although northwestern SCS basement is featured by single or major confined Yanshanian peak as represented by studied samples (Fig. 5), it turns out that the basement provided extremely limited sediments into our study area. Beibu Gulf Basin lies relatively isolated and farther to the channel while middle-south Qiongdongnan basement has been deeply submerged, even been distributed with voluminous carbonate platforms around Xisha Uplift since early Miocene. Likewise, Shenhu Uplift to the northeast of Qiongdongnan Basin was no more sediment supplier under the transgressional sedimentary environment during this time.

Nevertheless, QW1-2 and QE-2 within Pliocene strata show a larger difference than their upper Miocene samples on U–Pb combinations, indicating both temporal and spatial provenance shiftings. Yanshanian and Indosinian populations become dominant implying increased input from Hainan Island. By contrast, Caledonian clusters have been weakened into a relatively smaller scale for Pliocene samples, suggestive of decreasing trend in Central Vietnam supplement after late Miocene. Overall, age spectra become wider for both samples with higher abundance in Lvliangian clusters. Implication could be made that potential sources with more old Proterozoic zircons were also supplying sediments into Central Canyon. From west to east, QE-2 dominated by major peaks representing Yanshanian and Indosinian events is totally distinctive from QW1-2. This further confirms greater significance of Hainan Island than Central Vietnam when sediments were being transported eastwards along the entire course.

REE patterns tracing mafic-to-ultramafic sediment signals also display an evident spatial variation within the whole Central Canyon (Fig. 4). Since QW3-2 at the original point lies rather close to the Vietnamese margin, continual and abundant basic supplements were being dumped in this area resulting in intensive Eu enrichment from late Miocene to Pliocene. However, for the farther east well QW1, Hainan Island casted its influence on sample QW1-2 with more acidic sediments, hence modest-to-slight positive Eu anomalies even negative values were initially generated. As for the easternmost borehole of QE, basic material signal might have already been diluted to such a large extent that only one average data (3070–3168 m) of slight positive Eu anomaly was observed accompanied by other apparent negative values during late Miocene. Since Pliocene, Hainan Island exerted a dominant influence on QE-2 with large abundance of acidic transport that its REE patterns have all been replaced by obvious negative Eu anomalies. To make it more explicit, being situated at the western margin of Qiongdongnan Basin, QW2 might have been initially influenced by Hainan Island since late Miocene due to its special location leading to the dominance of negative Eu anomalies. Based on this unbalanced distribution pattern of positive Eu anomalies, we could further confirm that provenances surrounding the Central Canyon–Central Vietnam or Hainan Island as major potential sources—have been providing mafic-to-ultramafic or acidic sediments with different abundance largely at a temporal as well as a spatial scale (Fig. 6).

Conclusion

Constraints from detrital zircon U–Pb chronological analysis and REE geochemical results together generated a well-defined relationship between potential provenances and upper Miocene–Pliocene sediments in the Central Canyon. The collision orogenic belt between Indochina block and South China continent located in the Kontum Massif of the Central Vietnam has exerted significant influence on the sedimentary infilling processes of the Central Canyon in the northern SCS. The typical wide U–Pb spectra are identified by broad Indosinian, Caledonian and Jinningian clusters in the western studied samples. Correspondingly, the ophiolite suites generated during the late Triassic period has supplied mafic-to-ultramafic sediments into the Central Canyon course resulting in positive Eu anomaly signals. On the other hand, as another crucial potential contributor, Hainan Island featured by bimodal U–Pb combination also supply eastern samples with abundant terrigenous input, resulting in dominant Yanshanian and Indosinian peaks over other older-age zircon groups. In addition, different from basic sediment supplier of Central Vietnam, Hainan Island has dumped large abundance of acidic materials into its surrounding areas as well as the further western part of Qiongdongnan Basin. As

facilitated evidence, REE geochemical results tracing the entire channel provide a clearer explanation of the spatial changes in basic sediment signal distribution patterns. Conclusively, in the western region of Central Canyon, its sedimentary infilling processes have been largely under control by the provenance of Central Vietnam. By contrast, the eastern Central Canyon has gradually tended to be affected from Hainan Island after late Miocene. Overall at a time scale, for the sedimentary evolution of Central Canyon even the entire northwestern SCS basins, it is also implied that influences of Central Vietnam have been remarkably weakened and stepwise replaced by Hainan Island to the north.

Acknowledgements We thank China National Offshore Oil Corporation (CNOOC) for providing geological data and borehole samples from the northern South China Sea. Funding of this work was provided by the National Natural Science Foundation of China (Project Nos. 41576059, 91528301) and was also supported by the Fundamental Research Funds for the Central Universities and State Key Laboratory of Marine Geology (MG20180101). Reviewers offered critical comments and suggestions, which greatly improved this work.

References

Andersen T (2002) Correction of common lead in U–Pb analyses that do not report 204 Pb. Chem Geol 192:59–79

Antobreh AA, Krastel S (2006) Morphology, seismic characteristics and development of Cap Timiris Canyon, offshore Mauritania: a newly discovered canyon preserved-off a major arid climatic region. Mar Pet Geol 23:37–59

Arzola RG, Wynn RB, Lastras G, Masson DG, Weaver PPE (2008) Sedimentary features and processes in the Nazaré and Setúbal submarine canyons, west Iberian margin. Mar Geol 250:64–88

Bayliss N, Pickering KT (2015) Transition from deep-marine lower-slope erosional channels to proximal basin-floor stacked channel–levée–overbank deposits, and syn-sedimentary growth structures, middle eocene banastón system, Ainsa Basin, Spanish Pyrenees. Earth Sci Rev 144:23–46

Boynton WV (1984) Cosmochemistry of the rare earth elements; meteorite studies. Elsevier Science Publication Cooporation, Amsterdam

Burrett C, Zaw K, Meffre S, Lai CK, Khositanont S, Chaodumrong P, Udchachon M, Ekins S, Halpin J (2014) The configuration of Greater Gondwana—evidence from LA ICPMS, U-Pb geochronology of detrital zircons from the Palaeozoic and Mesozoic of Southeast Asia and China. Gondwana Res 26:31–51

Cai GF, Shao L, Qiao PJ, Liang JS (2013) Marine transgression and evolution of depositional environment in the Paleogene strata of Qiongdongnan Basin, South China Sea. Acta Pet Sin 34:91–101 (**in Chinese with English abstract**)

Cao LC, Jiang T, Wang ZF, Zhang YZ, Sun H (2015) Provenance of Upper Miocene sediments in the Yinggehai and Qiongdongnan basins, northwestern South China Sea: evidence from REE, heavy minerals and zircon U–Pb ages. Mar Geol 361:136–146

Cao L, Shao L, Qiao P, Zhao Z, van Hinsbergen DJJ (2018) Early Miocene birth of modern Pearl River recorded low-relief, high-elevation surface formation of SE Tibetan Plateau. Earth and Planet Sci Lett 496:120–131

Carter A, Bristow CS (2015) Detrital zircon geochronology: enhancing the quality of sedimentary source information through improved methodology and combined U–Pb and fission-track techniques. Basin Res 12:47–57

Chen H, Xie XN, Guo JL, Su M, Zong KQ, Shang F, Huang W, Wang W, Shang ZL (2015) Provenance of Central Canyon in Qiongdongnan Basin as evidenced by detrital zircon U-Pb study of Upper Miocene sandstones. Sci China Earth Sci 58:1337–1349

Cherniak DJ, Watson EB (2001) Pb diffusion in zircon. Chem Geol 172:5–24

Clark MK, Schoenbohm LM, Royden LH, Whipple KX, Burchfiel BC, Zhang X, Tang W, Wang E, Chen L (2004) Surface uplift, tectonics, and erosion of eastern Tibet from large-scale drainage patterns. Tectonics 23:TC1006. https://doi.org/10.1029/2002TC001402

Clift P, Carter A, Campbell I, Pringle M, Van Lap N, Allen C, Hodges K, Tan M (2006) Thermochronology of mineral grains in the Red and Mekong Rivers, Vietnam: provenance and exhumation implications for Southeast Asia. Geochem Geophys Geosyst 7:123–129

Condie KC, Belousova E, Griffin WL, Sircombe KN (2009) Granitoid events in space and time: constraints from igneous and detrital zircon age spectra. Gondwana Res 15:228–242

Flecker R, Krijgsman W, Capella W, de Castro Martíns C, Dmitrieva E, Mayser JP, Marzocchi A, Modestou S, Ochoa D, Simon D, Tulbure M, van den Berg B, van der Schee M, de Lange G, Ellam R, Govers R, Gutjahr M, Hilgen F, Kouwenhoven T, Lofi J, Meijer P, Sierro FJ, Bachiri N, Barhoun N, Alami AC, Chacon B, Flores JA, Gregory J, Howard J, Lunt D, Ochoa M, Pancost R, Vincent S, Yousfi MZ (2015) Evolution of the Late Miocene Mediterranean Atlantic gateways and their impact on regional and global environmental change. Earth Sci Rev 150:365–392

Fyhn M, Boldreel LO, Nielsen LH (2009) Geological development of the Central and South Vietnamese margin: implications for the establishment of the South China Sea, Indochinese escape tectonics and Cenozoic volcanism. Tectonophysics 478:184–214

Gong CL, Wang YM, Zhu WL, Li WG, Xu Q, Zhang JM (2011) The Central Submarine Canyon in the Qiongdongnan Basin, northwestern South China Sea: architecture, sequence stratigraphy, and depositional processes. Mar Pet Geol 28:1690–1702

Hale RP, Ogston AS, Walsh JP, Orpin AR (2014) Sediment transport and event deposition on the Waipaoa River shelf, New Zealand. Cont Shelf Res 86:52–65

Haq BU (1988) Mesozoic and Cenozoic chronostratigraphy and cycles of sea-level changes: an integrated approach, pp 71–108

Harris PT, Whiteway T (2011) Global distribution of large submarine canyons: geomorphic differences between active and passive continental margins. Mar Geol 285:69–86

He YL, Xie XN, Kneller BC, Wang ZF, Li XS (2013) Architecture and controlling factors of canyon fills on the shelf margin in the Qiongdongnan Basin, northern South China Sea. Mar Pet Geol 41:264–276

Horton BK, Hassanzadeh J, Stockli DF, Axen GJ, Gillis RJ, Guest B, Amini A, Fakhari MD, Zamanzadeh SM, Grove M (2008) Detrital zircon provenance of Neoproterozoic to Cenozoic deposits in Iran: implications for chronostratigraphy and collisional tectonics. Tectonophysics 451:97–122

Jobe ZR, Lowe DR, Uchytil SJ (2011) Two fundamentally different types of submarine canyons along the continental margin of Equatorial Guinea. Mar Pet Geol 28:843–860

Kesselmans RPW, Wijnberg JBPA., Groot AD, Vries NKD (2001) Understanding Mesozoic accretion in Southeast Asia: significance of Triassic thermotectonism (Indosinian orogeny) in Vietnam. Geology 29:211–214

Kosler J (2003) Present trends and the future of zircon in geochronology: laser ablation ICPMS. Rev Mineral Geochem 53:243–275

Leloup PH, Lacassin R, Tapponnier P, Schärer U, Zhong D, Liu X, Zhang L, Ji S, Trinh PT (1995) The Ailao Shan-Red River shear

zone (Yunnan, China), Tertiary transformboundary of Indochina. Tectonophysics 251(3–10):13–84
Li ZX, Li XH, Chung SL, Lo CH, Xu XS, Li WX (2012) Magmatic switch-on and switch-off along the South China continental margin since the Permian: transition from an Andean-type to a Western Pacific-type plate boundary. Tectonophysics 532–535:271–290
Li QY, Wu GX, Zhang LL, Shu Y, Shao L (2016) Paleogene marine deposition records of rifting and breakup of the South China Sea: an overview. Sci China Earth Sci 60:1–13
Li C, Lv CF, Chen GJ, Zhang GC, Ma M, Shen HL, Zhao Z, Guo S (2017a) Source and sink characteristics of the continental slope-parallel Central Canyon in the Qiongdongnan Basin on the northern margin of the South China Sea. J Asian Earth Sci 134:1–12
Li C, Ma M, Lv CF, Zhang GC, Chen GJ, Yan YK, Bi GX (2017b) Sedimentary differences between different segments of the continental slope-parallel Central Canyon in the Qiongdongnan Basin on the northern margin of the South China Sea. Mar Pet Geol 88:127–140
Liu YS, Gao S, Hu ZC, Gao CG, Zong KQ, Wang DB (2010) Continental and oceanic crust recycling-induced melt–peridotite interactions in the trans-north China orogen: U–Pb dating, Hf isotopes and trace elements in zircons from mantle xenoliths. J Petrol 51:537–571
Liu HC, Wang YJ, Cawood PA, Fan WM, Cai YF, Xing XW (2015) Record of Tethyan ocean closure and Indosinian collision along the Ailaoshan suture zone (SW China). Gondwana Res 27(3):1292–1306
Ma M, Li C, Lv CF, Chen GJ, Yang F, Yan YK, Yin N, Zhang GC (2016) Geochemistry and provenance of a multiple-stage fan in the Upper Miocene to the Pliocene in the Yinggehai and Qiongdongnan basins, offshore South China Sea. Mar Pet Geol 79:64–80
Mayall M, Jones E, Casey M (2006) Turbidite channel reservoirs—key elements in facies prediction and effective development. Mar Pet Geol 23:821–841
Mclennan SM (1989) Rare earth elements and sedimentary rocks: influence of provenance and sedimentary processes. Rev Miner 21:169–200
Mi LJ, Zhang GC (2011) Investigation and evaluation of oil and gas resources strategy. Geological Publishing House, Beijing (**in Chinese**)
Milliman JD, Farnsworth KL (2011) River discharge to the coastal ocean—a global synthesis. Cambridge University Press, New York
Moecher DP, Samson SD (2006) Differential zircon fertility of source terranes and natural bias in the detrital zircon record: implications for sedimentary provenance analysis. Earth Planet Sci Lett 247:252–266
Morton AC, Claoué-Long JC, Hallsworth CR (2001) Zircon age and heavy mineral constraints on provenance of North Sea Carboniferous sandstones. Mar Pet Geol 18:319–337
Mountjoy JJ, Barnes PM, Pettinga JR (2009) Morphostructure and evolution of submarine canyons across an active margin: Cook Strait sector of the Hikurangi Margin, New Zealand. Mar Geol 260:45–68
Popescu I, Lericolais G, Panin N, Normand A, Dinu C, Drezen EL (2004) The Danube submarine canyon (Black Sea): morphology and sedimentary processes. Mar Geol 206:249–265
Rangin C, Klein M, Roques D, Le Pichon X (1995) The Red River fault system in the Tonkin Gulf, Vietnam. Tectonophysics 243:209–222
Reimchen AP, Hubbard SM, Stright L, Romans BW (2016) Using seafloor morphometrics to constrain stratigraphic models of sinuous submarine channel systems. Mar Pet Geol 77:92–115
Rossi C, Kälin O, Arribas J, Tortosa A (2002) Diagenesis, provenance and reservoir quality of Triassic TAGI sandstones from Ourhoud field, Berkine (Ghadames) Basin, Algeria. Mar Pet Geol 19:117–142
Shao L, Li A, Wu GX, Li QY, Liu CL, Qiao PJ (2010) Evolution of sedimentary environment and provenance in Qiongdongnan Basin in the Northern South China Sea. Acta Pet Sin 31:548–552 (**in Chinese with English abstract**)
Shao L, Cao L, Pang X, Jiang T, Qiao P, Zhao M (2016) Detrital zircon provenance of the Paleogene syn-rift sediments in the northern South China Sea. Geochem Geophys Geosystems 17(2):255–269
Shao L, Meng A, Li Q, Qiao P, Cui Y, Cao L, Chen S (2017) Detrital zircon ages and elemental characteristics of the Eocene sequence in IODP Hole U1435A: implications for rifting and environmental changes before the opening of the South China Sea. Mar Geol 394:39–51
Sláma J, Kostler J, Condon DJ, Crowley JL, Gerdes A, Hanchar JM, Horstwood MSA, Morris GA, Nasdala L, Norberg N, Schaltegger U, Schoene B, Tubrett M, Whitehouse MJ (2008) Pleŝovice—a new natural reference material for U-Pb and Hf isotopic analysis. Chem Geol 249:1–35
Su M, Xie XN, Wang ZF, Jiang T, Zhang C, He YL (2013) Sedimentary evolution of the central canyon system in Qiongdongnan Basin, northern South China Sea. Acta Pet Sin 34(3):467–478 (**in Chinese with English abstract**). https://doi.org/10.7623/syxb201303007
Su M, Xie XN, Xie YH, Wang ZF, Zhang C, Jiang T, He YL (2014) The segmentations and the significances of the Central Canyon System in the Qiongdongnan Basin, northern South China Sea. J Asian Earth Sci 79:552–563
Taylor B, Hayes DE (1983) Origin and history of the South China Sea basin. In: Hayes DE (ed) The tectonic and geologic evolution of southeast Asian seas and islands: part 2. American Geophysical Union, Washington, D.C., pp 23–56
Trung NM, Tsujimori T, Itaya T (2006) Honvang serpentinite body of the Song Ma fault zone, Northern Vietnam: a remnant of oceanic lithosphere within the Indochina-South China suture. Gondwana Res 9(1–2):225–230
Usuki T, Lan CY, Yui TF, Iizuka Y, Vu TV, Tran TA, Okamoto K, Wooden JL, Liou JG (2009) Early Paleozoic medium-pressure metamorphism in central Vietnam: evidence from SHRIMP U-Pb zircon ages. Geosci J 13:245–256
Van Hoang L, Wu FY, Clift PD, Wysocka A, Swierczewska A (2009) Evaluating the evolution of the Red River system based on in situ U-Pb dating and Hf isotope analysis of zircons. Geochem Geophys Geosyst 10:292–310
Van Hoang L, Clift PD, Schwab AM, Huuse M, Nguyen DA, Zhen S (2010) Large-scale erosional response of SE Asia to monsoon evolution reconstructed from sedimentary records of the Song Hong-Yinggehai and Qiongdongnan basins, South China Sea. Geol Soc Lond Spec Publ 342:219–244
Vermeesch P (2012) On the visualisation of detrital age distributions. Chem Geol 312–313:190–194
Wang C, Liang XQ, Xie YH, Tong CX, Pei JX, Zhou Y, Jiang Y, Fu JG, Dong CG, Liu P (2014) Provenance of Upper Miocene to Quaternary sediments in the Yinggehai-Song Hong Basin, South China Sea: evidence from detrital zircon U–Pb ages. Mar Geol 355:202–217
Wang C, Liang X, Zhou Y, Fu J, Jiang Y, Dong C, Xie Y, Tong C, Pei J, Liu P (2015) Construction of age frequencies of provenances on the eastern side of the Yinggehai Basin: studies of LA-ICP-MS U-Pb ages of detrital zircons from six modern rivers, western Hainan China. Earth Sci Front 22:277–289 (**in Chinese with English abstract**)
Wiedenbeck M, Alle P, Corfu F, Griffin WL, Meier M, Oberli F, Quadt AV, Roddick JC, Spiegel W (1995) Three natural zircon standards for U-Th-Pb, Lu-Hf, trace element and REE analyses. Geostand Newsl 19:1–23

Xie XN, Müller RD, Li ST, Gong ZS, Steinberger B (2006) Origin of anomalous subsidence along the Northern South China Sea margin and its relationship to dynamic topography. Mar Pet Geol 23:745–765

Xie XN, Dietmar MR, Ren JY, Jiang T, Zhang C (2008) Stratigraphic architecture and evolution of the continental slope system in offshore Hainan, northern South China Sea. Mar Geol 247:129–144

Xu Y, Sun Q, Cai G, Yin X, Chen J (2014) The U-Pb ages and Hf isotopes of detrital zircons from Hainan Island, South China: implications for sediment provenance and the crustal evolution. Environ Earth Sci 71:1619–1628

Yan P, Deng H, Liu H, Zhang Z, Jiang Y (2006) The temporal and spatial distribution of volcanism in the South China Sea region. J Asian Earth Sci 27:647–659

Yan Y, Carter A, Palk C, Brichau S, Hu XQ (2011) Understanding sedimentation in the Song Hong–Yinggehai Basin, South China Sea. Geochem Geophys Geosyst 12:48–58

Yuan SQ, Lv FL, Wu SG, Yao GS, Ma YB, Fu YH (2009) Seismic stratigraphy of the Qiongdongnan deep sea channel system, northwest South China Sea. Chin J Oceanol Limnol 27:250–259

Zeng Z, Zeng X (1989) Physical Geography of Hainan Island. Science Press, Beijing (**in Chinese**)

Zhang C, Wang Z, Sun Z, Sun Z, Liu J, Wang Z (2013) Structural differences between the western and eastern Qiongdongnan Basin: evidence of Indochina block extrusion and South China Sea seafloor spreading. Mar Geophys Res 34:309–323

Zhang H, Shao L, Zhang GC, Chen SH, Wu GX (2015) Distribution and petroleum geologic significance of Eocene marine strata in the South China Sea. Earth Sci J China Univ Geosci 40:660–670 (**in Chinese with English abstract**)

Zhao M, Shao L, Liang JS, Li QY (2015) No Red River capture since the late Oligocene: geochemical evidence from the Northwestern South China Sea. Deep Sea Res II 122:185–194

Zhong ZH, Liu JH, Zhang DJ, He XH, Zhang YZ, Liu XY, You L, Liu XY (2013) Origin and sedimentary characteristics of a large submarine fan in Dongfang area, Yinggehai basin. Acta Pet Sin 34:102–111 (**in Chinese with English abstract**)

Zhu W, Lei C (2013) Refining the model of South China Sea's tectonic evolution: evidence from Yinggehai-Song Hong and Qiongdongnan Basins. Mar Geophys Res 34:325–339

Zhu M, Graham S, McHargue T (2009) The Red River Fault zone in the Yinggehai Basin, South China Sea. Tectonophysics 476(3–4):397–417

Zhu WL, Xie XN, Wang ZF, Zhang DJ, Zhang CL, Cao LC, Shao L (2017) New insights on the origin of the basement of the Xisha Uplift, South China Sea. Sci China Earth Sci 60:1–9